Journal of Advanced Manufacturing Systems
(2026) 1–25

DOI: 10.1142/S0219686727500430

Temperature Stabilized Vibration-Based Condition Monitoring of Machine Tool Spindles

Mohammad Mudhasir* and Mohit Law †

Machine Tool Dynamics Laboratory
Department of Mechanical Engineering
Indian Institute of Technology Kanpur
Kanpur 208016, Uttar Pradesh, India
**mudhasir315@gmail.com*
†mlaw@iitk.ac.in

Received 2 November 2025
Accepted 26 December 2025
Published 10 January 2026

Temperature has a strong influence on spindle vibration behavior, yet most vibration-based condition-monitoring practices do not account for thermal stabilization. Through controlled measurements on two representative spindle systems — a naturally cooled high-speed electro-spindle and an oil-cooled direct-drive spindle — this study demonstrates that vibration RMS levels and defect-related spectral features can change by up to 40–87% from cold-start to thermal steady state. To address this, we introduce the *thermal time constant* as a quantitative and robust metric for identifying when a spindle has reached temperature-stabilized operating conditions. First-order exponential fits to housing temperature measurements show that τ decreases with spindle speed and differs significantly across spindle types, reflecting differences in thermal mass and cooling effectiveness. Spectral analysis further reveals that peak defect magnitudes stabilize only after approximately 2τ–3τ, matching trends seen in RMS stabilization. Using τ therefore enables reliable prescription of warm-up times and prevents misclassification of temperature effects as health degradation. The proposed framework provides a practical, measurement-driven approach for establishing temperature-stabilized vibration monitoring protocols for diagnostics and prognosis.

Keywords: Spindle; condition monitoring; vibration; temperature; spectral analysis.

1. Introduction

The performance of a machine tool is governed by its spindle.[1] Monitoring the spindle's health is important to plan its maintenance and to avoid part rejections. Monitoring also plays a key role in the development of smart and autonomous Industry 4.0 solutions.[2] Health monitoring of spindles is done by monitoring their vibration levels, which serve as a proxy for health.[3,4] Since vibration levels at

†Corresponding author.

cold-start are very different than when the spindle has thermally stabilized, it is important to establish temperature-stabilized monitoring protocols. Surprisingly, no such protocols exist. Some reports recommend running the machine through a warm-up cycle before measuring vibrations.[5–7] Defining warm-up cycles is challenging due to their variability across spindle types (drive, design, cooling mechanisms, bearing arrangements, power and size) and application contexts, making a universal protocol impractical. This underscores the need for a robust, quantifiable metric to identify when a spindle has reached thermal stability. Such a metric would enable consistent and reliable vibration-based diagnostics by isolating health-related changes from temperature-induced effects. This paper aims to contribute toward the development of such a metric to support diagnostic and prognostic measurements in spindle systems.

Spindle systems are complex assemblies of rotating and non-rotating parts. Relative motion between these parts generates frictional heating. That heat not only results in thermal expansion-related errors of the spindle system, but also changes the vibration signatures. Though there is much research reported on how thermal expansion manifests as a deviation/error in the tool's position,[8–10] the research relating temperature changes to changes in vibration levels is limited.[11] Even in that report, though changes in temperatures and vibrations with time were reported, there was no correlation of vibrations changing with temperatures. Related reports have documented how the dynamics of spindle systems change with temperature.[12] However, that report too did not characterize how vibrations change with temperature.

To address the need for directly correlating how vibrations change with temperature, we propose the evaluation of a thermal time constant to serve as a robust new metric for temperature and vibration stabilization. We define the thermal time constant herein as the time the spindle system takes to reach 63.2% of its steady-state operating temperature. In this sense, the thermal time constant is like the time constant for the step response of a first-order system.[13] Since machine tool spindles have been reported to behave like first-order systems,[14] we think the use of the thermal time constant is valid. The proposed constant characterizing temperature and vibration stabilization is the first of two new technical contributions of this work.

We illustrate the evaluation of a thermal time constant with measurements on two representative spindles. One is a high-speed, naturally cooled electro-spindle mounted on a test bench, and the other is a direct-driven driven oil-cooled spindle mounted on a CNC machine. Since one spindle is motorized and naturally cooled, and since the other is directly driven and oil-cooled, the spindle types are thought to be representative of the wide spectrum of all available spindles. Furthermore, to isolate how vibrations change with temperatures, and not how these potentially change with damage in the spindle system, the spindles we used had no damage. Moreover, we clarify that the methods and analysis we present are meant to characterize the behavior of the spindle in laboratory settings and are not meant for real-time implementation in factory settings. The aim is to help establish a practical guideline that can recommend spindle warm-up procedures before vibration measurements are undertaken for diagnostics and/or prognostic reasons.

The second new contribution is to characterize temperature-stabilized spectral behavior. Vibration-based condition monitoring aims to diagnose defects and predict the remaining useful life of spindle systems. ISO standards[3,4] recommend monitoring the root mean square (RMS) of measured vibrations. However, RMS values offer limited utility for diagnostic or prognostic purposes. As a result, spectral methods are preferred for condition assessment and fault detection.[6,7,15–17] As spindles with defects rotate, different defects cause different periodic impulses. The usual method to diagnose defects is to search for their corresponding frequencies from within the Fourier spectrum of the measured vibration signal.[16,17] For prognostics, the magnitudes of the defect peaks are tracked to evaluate if they cross a pre-specified threshold.[7,16] However, since peak magnitudes change with running time and temperature, a robust prognostic system must be able to distinguish temperature effects from degradation effects. To facilitate such analysis, this paper presents an analysis to help characterize how the spectral behavior changes with temperature, which in turn changes with run time.

We take this opportunity to clarify that it is not our aim to perform prognostics or even provide thresholds that can be used to check if there are defects in the bearing system. It is the modest goal of our paper to propose that measurements be taken for diagnostic analysis only after the spindle has thermally stabilized. We further clarify that if measurements for diagnostics are always taken after the spindle has thermally stabilized, then that measurement is potentially more trustworthy, since it eliminates cold-start effects. And, since the measurements will be more trustworthy, diagnostics and prognostics based on those measurements can be made more reliable.

The remainder of the paper is organized as follows. The experimental setups and plan are discussed in Sec. 2. Vibration levels changing with speed, and time/temperature are discussed in Sec. 3. Evaluation of the thermal time constant is discussed in Sec. 4. Section 5 discusses the time-and temperature-dependent spectral analysis. Section 6 discusses the generalizability of our methods as well as the limitations for practical implementation. The main conclusions and outlook follow in Sec. 7.

2. Experimental Setup and Plan

To characterize how vibrations change with speed, and time/temperature, we instrumented two spindles with thermocouples and accelerometers. The first spindle we measured was a new, naturally air-cooled motorized spindle that had a maximum speed of 24000 rpm, and its rated power was 0.8 kW — see Fig. 1(a) for its measurement setup. The total run-time on this spindle prior to experimentation was less than 10 h. The second spindle we measured was a directly driven spindle mounted on a 3-axis AMSL-made ACER model vertical CNC machine — see

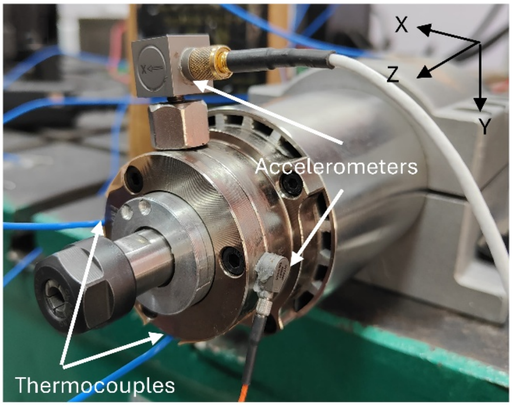

(a)

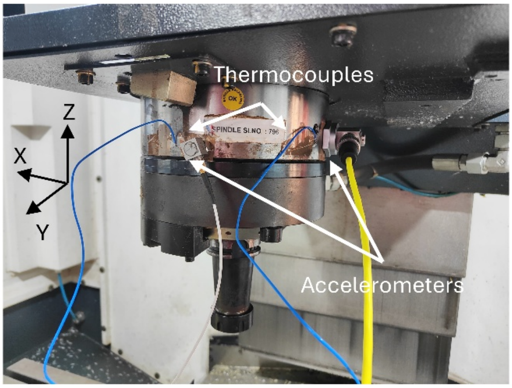

(b)

Fig. 1. Experimental setup to measure accelerations and temperatures of (a) a motorized 0.8 kW, 24000 rpm spindle mounted on a test bench, and (b) a directly driven 18 kW, 15000 rpm spindle mounted on a CNC machine.

Fig. 1(b) for its measurement setup. The second spindle is not new. However, its total run-time was less than 500 h, making this a relatively unused spindle. It should also be noted that both spindles had no obvious defects and were reported to be running fine.

Our measurement protocols were based on the ISO standard's guidelines[3,4] which recommend using balanced tool holders, placing the sensors near the bearing locations, and measuring at speeds at which the spindle will usually be operated. We also note here that all measurements were conducted in laboratory settings. For measuring accelerations, two piezoelectric-type accelerometers were mounted on the spindle housing near the front bearing locations. For measuring the motorized spindle, we used one Dytran make accelerometer with model number 32,251, and that had a sensitivity of 10 mV/g to measure response in the X-direction, and to measure response in the Y-direction, we used an Endevco make sensor with model number 44A16, which had a sensitivity of 100 mV/g. Measurements for this spindle were carried out at four different spindle speeds: 4800, 9600, 14700, and 19800 rpm. These speeds span the full working range of the spindle. And, for the spindle in the CNC machine, we used a Wilcoxon-made sensor with model number 785A, and a sensitivity of 100 mV/g to measure response in the X-direction, and the other was an Endevco-made sensor with model number 44A16, and a sensitivity of 100 mV/g to measure response in the Y-direction. For this spindle too, measurements were carried out at four different spindle speeds that covered the full operating speed range of this spindle type: 2000, 6000, 10000, and 15000 rpm.

Accelerations were acquired using a National Instruments' NI9234 data acquisition card mounted in a NI9171 chassis. All acceleration signals were acquired for 15 s durations at a sampling rate of 25.6 kHz. MATLAB's signal processing toolbox was used to acquire and process signals. Both spindles were cold-started and then continuously run at the speed of interest, and accelerations were measured at 5-min intervals for a total experimental duration of 60 min, i.e. we made 12 measurements over a period of 60 min. The spindles were allowed to cool down to room temperature before conducting experiments at another speed.

Along with measuring accelerations, we simultaneously recorded temperatures. Two K-type PT100 thermocouples were taped on the spindle housing near the accelerometer mounting locations, i.e. one in each direction. One additional thermocouple of the same type was used to monitor the ambient temperature. For monitoring temperatures, we used a Labart-made digital sensor (model number: HT-9815) which had thermocouples of the Tempsens make with model numbers of PCS-RTD-01, and with a sensitivity of 0.1 °C for temperatures below 1000 °C. Since the temperature sensor had a digital display, we simply noted the temperature at the same time as measuring accelerations.

3. Vibrations Changing with Speed and Time/Temperature

This section presents results to show how vibrations change with speed and time/temperature. Since it is not possible to maintain a constant temperature, vibration changes with time alone could not have been investigated separately, and for the analysis presented, it should be noted that temperatures change with run time.

In the first sub-section herein, we outline how we processed signals, and the next two sub-sections present results for the motorized spindle and the directly driven spindle, respectively. The final sub-section discusses potential mechanisms that can explain the observed behavior. For both spindles, we analyze how vibrations change with time/temperature and speeds and also evaluate the percentage change in the vibration levels as compared to the cold-start condition, as well as the vibration levels at the previous time-step of measurement. The aim of characterizing the response with this second metric is to evaluate how long it takes for the vibrations to stabilize within a measurement band of ±10%. The ±10% limit is prescribed by Clause 8.1.1 of the ISO standards as an acceptable uncertainty in the measurements.[3,4]

3.1. *Signal processing and noise floors*

Measured accelerations were low-pass filtered using a fourth-order Butterworth filter with a cut-off frequency of 10 kHz. The cut-off frequency was selected based on guidelines in the ISO standards.[3,4] Then, to estimate the vibration RMS levels from the filtered signals, we sectioned the 15 s measured data into three parts of equal length and evaluated the RMS for each part and charted the mean and the variance of every measurement. No signal segmentation was applied. And, since the measured acceleration data showed no trends or drifts, detrending was not necessary.

The baseline vibration noise response (RMS) when the spindles were not rotating was evaluated to be ~0.015 m/s^2. And, since the RMS levels of the measured vibration signals were of the levels of ~1.5 m/s^2 or higher, the signal-to-noise ratio was of the order of 100 or more. The minimum observed changes in the RMS levels during measurements were of the order of 0.3 m/s^2 or more, i.e. the ratio of the changes in acceleration RMS levels to the noise floor was of the order of 10 or more, and as such, measurements and changes in them are clearly distinguishable from the noise floor. Moreover, since the acceleration sensors remained mounted on the spindles during all measurements, repeatability-related uncertainties due to remounting the sensors were not faced.

Measured temperatures, too, did not exhibit any drift, and as such, no drift correction was applied for the measured temperatures. The noise floor for the temperature measurements was of the order of the sensitivity of the thermocouple, i.e. 0.1°C for temperatures below 1000°C.

3.2. *Behavior of the motorized spindle mounted on the test bench*

Vibration RMS levels changing with speed and time/temperature are shown in Fig. 2, and the percentage change in vibration levels is shown in Fig. 3.

As is evident from Fig. 2, the reference ambient temperature showed a slight increase over the measured time duration of 60 min. The laboratory's temperature not being controlled using forced cooling can explain this slight rise. Figure 2 also clearly shows that the variation in the RMS levels for each measurement is negligible (<1%), indicating good repeatability. Moreover, since this spindle was mounted on a test bench, influences of asymmetrical boundary conditions are expected to be less, and as such, we observed negligible differences between the X- and Y-directional responses.

In general, we observe that vibration levels increase with speed and with time/temperature. We also observed that higher speeds resulted in higher steady-state temperatures. For the speed of 4800 rpm, results for which are shown in Fig. 2(a), the temperature rise over the 60-min duration was around 5°C. For 9600 rpm,

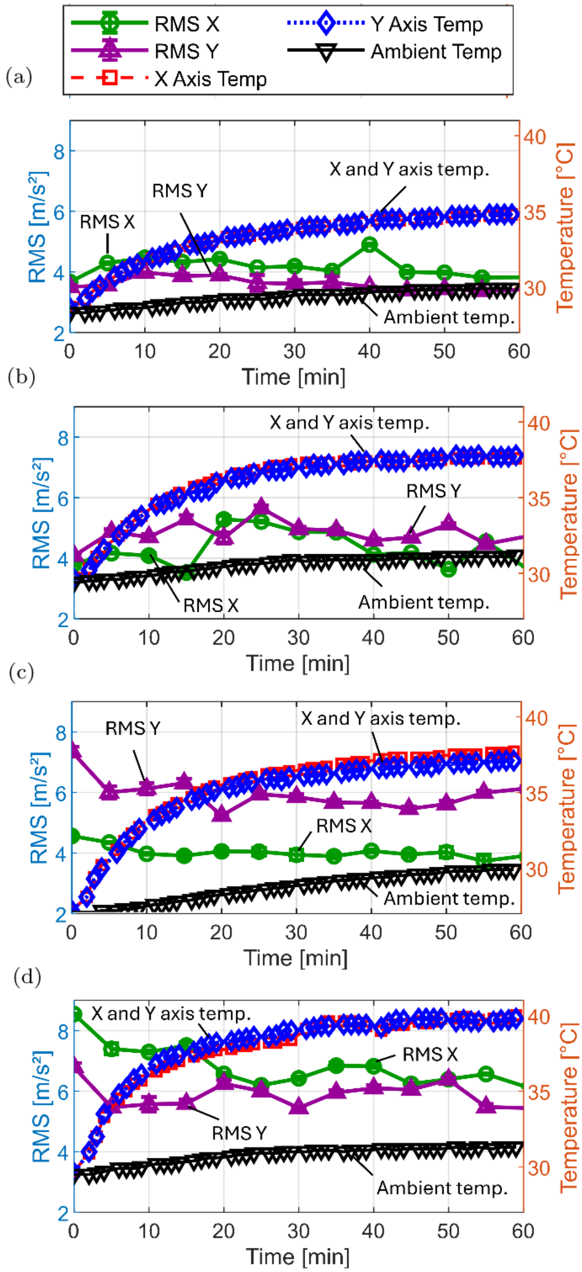

Fig. 2. Vibration levels of the motorized spindle mounted on a test bench changing with time and temperature for different speeds: (a) behavior at 4800 rpm, (b) behavior at 9600 rpm, (c) behavior at 14700 rpm, and (d) behavior at 19800 rpm.

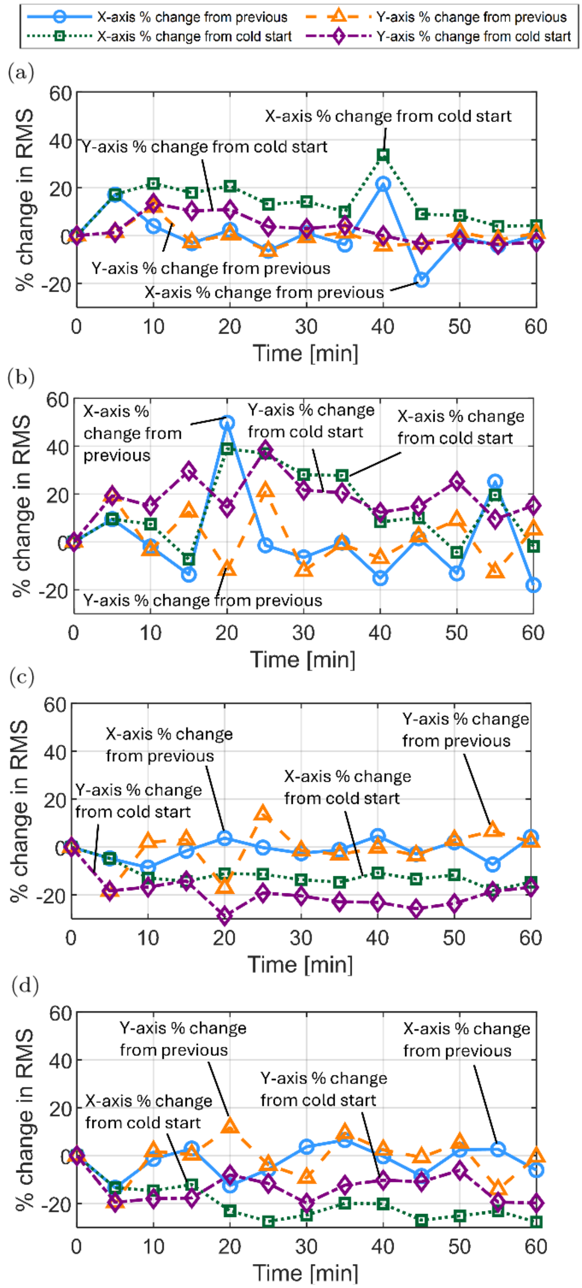

Fig. 3. Percentage change in vibration RMS levels of the motorized spindle mounted on a test bench, changing with respect to cold start and with respect to the measurement at the previous time step: (a) behavior at 4800 rpm, (b) behavior at 9600 rpm, (c) behavior at 14700 rpm, and (d) behavior at 19800 rpm.

it was around 6.5°C — see Fig. 2(b). For 14700 rpm, it was around 7.5°C — see Fig. 2(c), and for 19800 rpm, it was around 8.5°C — see Fig. 2(d). For the speed of 4800 rpm, the increase in the X-directional vibration RMS level is around 35% when compared to the cold-start condition — see Fig. 3(a). And, when compared to the vibration levels of the previous time step's measurement, the RMS levels appear to stabilize to be within the acceptable ±10% limit in between 10 min and 15 min of run time. Though there appears to be a sudden and abrupt increase in RMS levels between 40 min and 45 min, the RMS levels again stabilize. Likewise, for the speed of 9600 rpm, results for which are shown in Fig. 3(b), though there are times at which the RMS levels in the X- and Y-directions increase by around 40% as compared to their cold start conditions, the RMS levels in both directions eventually settle to be within the acceptable ±10% limit after around 25 min of run time.

Unlike the increase in the RMS levels as compared to the cold start conditions for operations at speeds of 4800 rpm and 9600 rpm, for experiments at the speeds of 14700 rpm and 19800 rpm, results for which are shown in Figs. 2(c), 2(d), 3(c), and 3(d), respectively, there is a reduction in the RMS levels as compared to the cold start condition. The change with respect to the cold start conditions for both these higher speeds is also less, at around 25%. And, for both these speeds, the vibration levels when compared to their previous measured state, stabilize to be within the acceptable ±10% limit in between 20 min and 30 min of run time.

Since the change in measured RMS levels from cold-start conditions to temperature stabilized conditions is as much as 40%, it is likely that if temperature stabilized vibration monitoring protocols are not followed, then misclassification of the spindle's health is possible. Since it appears that vibration levels stabilize around the same time as temperatures, to establish a temperature-stabilized vibration monitoring protocol, we propose to use the thermal constant evaluation of which is discussed in Sec. 4.

3.3. *Behavior of the direct-driven spindle mounted on the CNC machine*

Vibration RMS levels changing with speed and time/temperature for this spindle are shown in Fig. 4, and percentage change in vibration levels are shown in Fig. 5. As is evident from Fig. 4, the reference ambient temperature for this spindle does not vary much over the duration of the experiments, and nor does the reference ambient temperature change much for operation at different speeds. This is likely due to experiments being conducted in a controlled laboratory setting. Figure 4 also clearly shows that the variance in the RMS levels for each measurement is negligible (<1%), indicating good repeatability.

When the operational speed is 2000 rpm, results for which are shown in Fig. 4(a), the temperature of the spindle housing in the X- and Y-directions increases only by around 1°C. Though the temperature does not change by very much, the RMS levels after 60 min of running reduce by around 20% when compared to the RMS

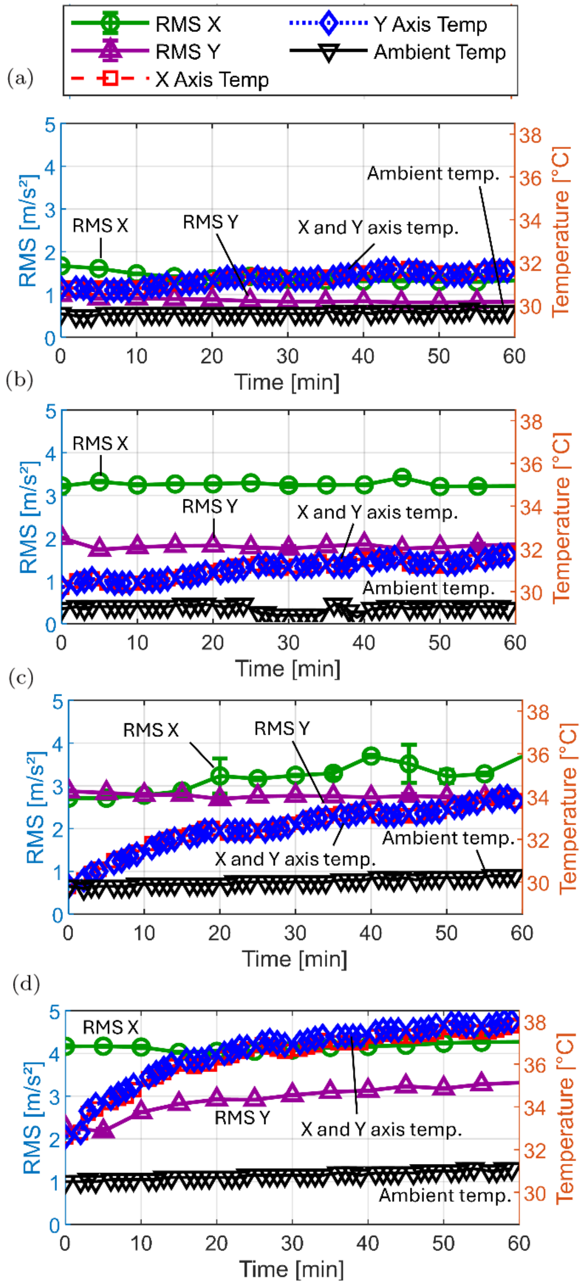

Fig. 4. Vibration levels of the direct drive spindle mounted on the CNC machine changing with time and temperature for different speeds: (a) behavior at 2000 rpm, (b) behavior at 6000 rpm, (c) behavior at 10000 rpm, and (d) behavior at 15000 rpm.

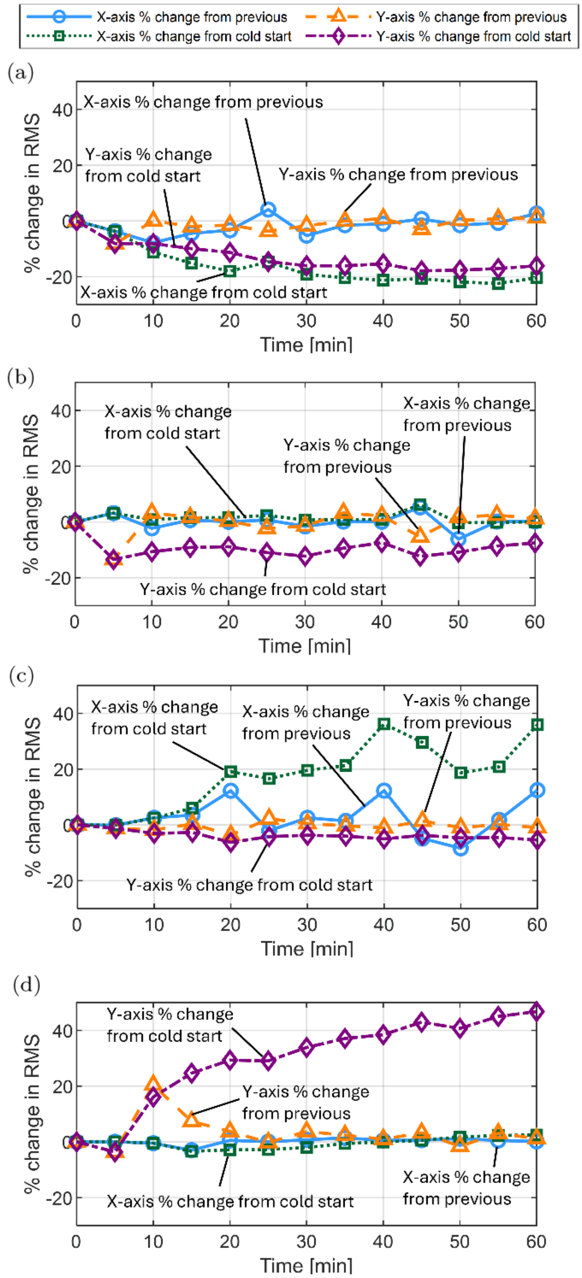

Fig. 5. Percentage change in vibration RMS levels of the direct drive spindle mounted on the CNC machine changing with respect to cold start and with respect to the measurement at the previous time step: (a) behavior at 2000 rpm, (b) behavior at 6000 rpm, (c) behavior at 10000 rpm, and (d) behavior at 15000 rpm.

levels at the cold-start condition — see Fig. 5(a). This is larger than the ±10% uncertainty that is deemed acceptable. However, when the percentage change in RMS levels from the previous time step is compared, the vibration levels appear to stabilize within ±10% between 10 min and 15 min of the running of the spindle.

For measurements at the rotational speed of 6000 rpm, results for which are shown in Figs. 4(b) and 5(b), respectively, even though there is a slight increase in temperature of the spindle housing with measurement time, the change in RMS levels of vibrations in the X-direction remains within the acceptable ±10%. However, for the Y-direction, the change with respect to the cold-start condition is around 15%. This settles to be within ±10% of the previous time's measurement within 10–15 min of running the spindle. The difference between the X- and Y-directional vibration levels can be explained by the spindle housing and machine not being symmetrical.

When the spindle is run at 10000 rpm, results for which are shown in Figs. 4(c) and 5(c), respectively, the temperature in both directions increases by around 3.5°C in the first 30 min and then appears to stabilize for the remainder of the 30 min of the operation. The X-directional vibration levels increase by around 40% from the cold-start condition and stabilize to be within ±10% of the previous time's measurement after running the spindle for around 15 min.

Similar behavior is observed for running the spindle at 15000 rpm, the results for which are shown in Figs. 4(d) and 5(d), respectively. In this case, the temperature increased by around 4°C in the first 30 min, and the temperature then stabilized over the next 30 min. For the 15000 rpm experiments, the measured Y-direction vibrations follow the temperature trend. Oddly, there is no significant change in the vibrations in the other directions. However, the change in the RMS levels of vibrations in the directions that follow the temperature change behavior is around 40% when benchmarked with respect to the cold-start condition. Interestingly, at higher speeds, the vibration levels increase with run time as compared to the cold-start condition. However, at lower speeds, the vibration levels after 60 min of run time were observed to be lower than those of the cold-start condition. If, however, the change of vibration levels from its previous state is evaluated, then it appears that the RMS levels stabilize to be within ±10% at around 15 min of running the spindle.

Since the measured RMS levels for this spindle also change by as much as 40% from cold-start, a temperature-stabilized vibration monitoring protocol is necessary. We therefore propose using the thermal constant for this purpose. The value of τ for this spindle type is also evaluated and discussed in Sec. 4.

3.4. *Discussions on the potential mechanisms to explain observed trends*

Prior to presenting methods to evaluate the thermal time constant, we discuss herein potential mechanisms that explain the observed trends of vibrations changing with speed and time/temperature.

Vibrations increasing with speed are normal and expected. Any imbalance in the spindle system due to defects and eccentricities from the manufacturing and assembly procedures will result in an unbalanced force. This force will increase with increasing speeds.[1] And, when forced excitations are of higher levels, the response, i.e. vibration levels too, will be higher. Hence, vibration levels with speed are given. The aim is hence to characterize temperature-related changes.

In general, relative motion between the rotating and non-rotating parts of a spindle system generates frictional heating. The heat generated increases with the speed of rotation.[18] And, since spindle systems are made of metallic parts, the parts tend to expand with a rise in temperature. The expansion, in turn, results in thermal softening of the bearings.[12] We hypothesize that the softening of bearings reduces the vibration signatures, and this might help explain why we see a reduction in vibration RMS levels as temperatures increase for runs at most speeds. Softening will also likely result in a change of bearing preloads. However, since the relationship between preload levels and vibrations is complex and not fully understood yet, the vibration levels do not always reduce monotonically. We see one case in which vibrations increase with an increase in temperature — see the case of the spindle in the CNC machine being run at a speed of 15000 rpm, results for which are shown in Fig. 4(d).

The increase in vibration levels could also be partially explained by how frictional heating results in a reduction of the viscosity of the grease lubricating the bearings.[19] The reduction in viscosity may result in unwanted contact between rolling elements and the inner/outer raceways of the bearings, and these may, in turn, result in impulse excitations, which could, in turn, increase the level of vibrations. Though a reduction in viscosities due to an increase in temperatures is expected to result in an increase in vibration levels, besides the case shown in Fig. 4(d), we did not see a consistent trend of vibrations increasing with time/temperature. A plausible explanation is that the maximum temperature increase observed over the 60-min duration was likely insufficient to induce a significant change in grease viscosity, thereby limiting any measurable effect on bearing vibration levels. Furthermore, tribological mechanisms resulting from a potential reduction in viscosities are complex and not fully understood and/or characterized yet. This could also explain why we do not always see changes as expected.

4. Evaluation of the Thermal Time Constants

Since vibration RMS levels depend strongly on temperature, we must identify when both temperature and vibration have stabilized, so that diagnostic measurements are taken only after this point. We propose to use the thermal time constant as that metric.

Assuming that the spindle assembly can be approximated as a lumped thermal system with some thermal resistance and thermal capacitance, when the spindle is switched on and operated at a constant speed, the transient temperature rise can be modeled as a first-order system[14]:

$$T(t) = T_f - (T_f - T_0)e^{-t/\tau}, \tag{4.1}$$

where in T_0 is spindle temperature at cold start, T_f is the temperature after stabilization, and τ is thermal time constant of the spindle system, which in turn is a function of the spindle's thermal resistance and thermal capacitance.

At $t = \tau$, Eq. (4.1) becomes as follows:

$$T(\tau) = T_f - 0.37(T_f - T_0). \tag{4.2}$$

This then becomes a measure of how quickly the spindle system responds to a change by reaching 63% of the total temperature rise. We propose to use this to quantify how the vibration RMS levels evolve along the thermal time scale. Naturally, a higher time constant indicates a slower response time.

To evaluate τ, we perform a nonlinear least-squares fit on the temperature time series data. For a representative X-directional measurement at a speed of 4800 rpm for the motorized spindle on the test bench, the data and the fit are shown in Fig. 6. The goodness of fit in this case, characterized by the R^2 value, is 0.99. This validates our assumption of an exponential first-order model being sufficient to describe the thermal characteristics of the system.

We also evaluated the 95% confidence intervals (CI) for this fit, and report those values in Table 1. That table also lists all the evaluated parameters for all speeds of interest for both spindle types of interest. In general, the R^2 values for all but the two low-speed measurements on the spindle on the CNC machine are above 0.95, suggesting that the first-order fit is indeed satisfactory.

In general, we observe that the τ reduces with an increase in speed. For the motorized spindle on the test bench, τ reduces from being ~15 min at 4800 rpm to ~10 min at 19800 rpm. And, for the spindle on the CNC machine, τ reduces from

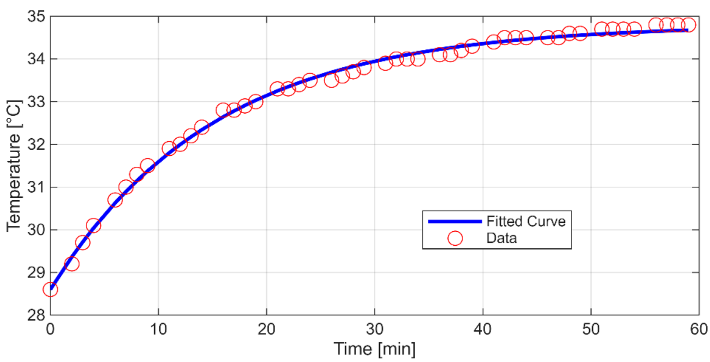

Fig. 6. Temperature time series data along with a data fit to estimate the thermal time constant for the case of a representative example of the X-directional measurement at a speed of 4800 rpm for the motorized spindle on the test bench.

Table 1. Summary of estimates for the thermal time constants with the goodness of fits and confidence intervals.

Motorized spindle on the test bench						
Speed	τ [min]		R^2		±95% CI [min]	
[rpm]	X	Y	X	Y	X	Y
4800	15.56	15.14	0.99	0.99	[15.31, 15.80]	[14.86, 15.41]
9600	11.53	13.02	0.99	0.99	[11.18, 11.87]	[12.76, 13.28]
14700	12.9	12.38	0.99	0.99	[12.64, 13.16]	[12.12, 12.64]
19800	11.98	9.78	0.97	0.98	[11.40, 12.56]	[9.41, 10.15]

Direct driven spindle on the CNC machine						
Speed	τ [min]		R^2		CI	
[rpm]	X	Y	X	Y	X	Y
2000	34.46	31.04	0.83	0.78	[30.05, 38.87]	25.78, 36.30
6000	33.09	29.82	0.85	0.9	[29.89, 36.29]	[27.42, 32.22]
10000	19.76	20.32	0.95	0.97	[18.68, 20.84]	[19.39, 21.24]
15000	16.87	15.89	0.98	0.99	[16.28, 17.46]	[15.40, 16.37]

being ~33 min at 2000 rpm to ~16 min at 15000 rpm. Since τ characterizes how "fast" the thermal system responds, τ being lower at higher speeds is consistent with the observed temperature stabilization for the two spindle types. We also observe τ to be different for both spindle types. Since the spindle in the CNC machine is larger than the test bench spindle, its thermal resistance and thermal capacitance are also larger. This explains why the estimates for τ, which depend on these parameters, are larger for the spindle on the CNC machine — despite the spindle on the CNC machine being oil-cooled. We also observe the estimates of τ not being very sensitive to the direction of temperature measurement.

Our analysis suggests that if τ is to be used to prescribe a warm-up time before taking condition-monitoring vibration measurements, and if it is desired that measurements be taken when the temperature has reached 63% of the final stabilized temperature, then a warm-up time of 1τ is sufficient. However, if, for example, it is desired that measurements be instead taken when the spindle temperature has reached 95% of its final stabilized temperature, then a warm-up time of 3τ might be more suitable. This and other such considerations for practical implementation are discussed in Sec. 6.

5. Time- and Temperature-dependent Spectral Analysis

The analysis in Secs. 3 and 4 characterizes how vibration RMS levels change with speed, and time/temperature. That analysis, though necessary for establishing thermal stabilization-based vibration monitoring guidelines, does not help in spindle diagnostics, i.e. temperatures and RMS levels do not reveal what, if anything, is damaged in the spindle system. In response to that need, this section presents time- and temperature-dependent spectral analysis that can help classify defects in the system, and that can track how those are also influenced by temperature changes.

For both spindles, we present results at representative high speeds and in representative directions. Our analysis at one speed and in one direction is typical of spectral analysis of spindle systems.[6,7,17] We first outline the spectral analysis procedures in Sec. 5.1, followed by analysis for the motorized spindle in Sec. 5.2, and for the spindle in the CNC machine in Sec. 5.3, respectively. In each sub-section, we first discuss the defects we can classify. That is followed by showing how the spectrum evolves over the measurement period of 60 min. We then track how the peak magnitude of one representative defect frequency that is classifiable in all measurements changes across the measurement period. The aim of such analysis is to evaluate and report whether the spectral behavior changing with time and temperature follows trends observed in the corresponding change in the RMS behavior.

5.1. *Spectral analysis procedures*

To obtain spectra, we perform a Fourier transform on the measured accelerations, which were low-pass filtered using a fourth-order Butterworth filter with a cut-off frequency of 10 kHz — as discussed already in Sec. 3.1. Apart from the low-pass filter, we also comb filtered the supply frequency and its harmonics. The spectra were computed directly from the time-domain signals without windowing. While window functions are commonly used to reduce spectral leakage, they also modify the amplitude and shape of spectral peaks, and as such, we avoid their use. Given that our records were 15 s long (frequency resolution $\approx$ 0.067 Hz), we chose not to apply averaging or segmentation. Since the measured acceleration data showed no trends or drifts, no de-trending was applied. Zero-padding was also not used, as it merely interpolates the fast-Fourier transform (FFT) bins without increasing actual frequency resolution. We acknowledge that some spectral leakage may remain because the measured vibration frequencies do not always contain an integer number of cycles within the 15 s window. Since the defect frequencies can vary widely, it was not feasible to adjust the sampling or duration to make all frequency ratios exact integers. The reported spectra should therefore be interpreted with these known limitations in mind.

To classify faults and defects using spectral analysis, we search for the known fault/defect peak signatures from within the spectra. Faults in the spindle systems, such as misalignments and looseness, have well-known spectral signatures. Misalignments are typically characterized by a peak in the spectrum at harmonics of the spindle rotational frequency, f_{Sp}, being of greater magnitudes than the peak magnitude at f_{Sp}. Looseness is typically characterized by peaks in the spectrum at sub-harmonics and fractional multiples of the spindle rotational frequency, f_{Sp}. Likewise, each type of bearing defect also has its own unique spectral signature. Inner, f_I and outer, f_O race defect frequencies capture the rate at which balls contact a defect in the raceway(s). The ball spin frequency, f_{B} characterizes a defect in the ball(s). The cage defect frequency, f_{B} also referred to as the fundamental train frequency, describes the rotating speed of the cage assembly. To evaluate these

Table 2. Bearing details along with their defect multipliers and frequencies for both spindle types. For evaluation of bearing defect frequencies, we relied on expressions given in Ref. 16.

Parameter	Motorized spindle	Direct driven spindle
Front bearing specification	7002C P4	70BNR10HTYNSULP4
Pitch diameter [mm]	23.5	90
Contact angle [°]	15	18
Number of balls	12	25
Ball diameter [mm]	4.762	8
Speed at which Fourier analysis is conducted (f_{Sp}) [Hz]	330 (19800 rpm)	250 (15000 rpm)
Outer race defect frequency (f_O) [Hz]	1593.9	2860
Inner race defect frequency (f_I) [Hz]	2366.1	3390
Rolling element defect frequency (f_{B}) [Hz]	1567.5	2792.5
Cage defect frequency (f_C) [Hz]	132	115

defect frequencies, we use well-established relationships that relate defect frequencies to bearing geometry, contact angle, number of balls, and the rotational speed.[15] Details of the two spindles and their defect frequencies at listed in Table 2.

No thresholding was applied for peak identification and/or classification. To classify compound defects, we carried out a search in a structured search space that included the four possible bearing defect frequencies along with their harmonics up to the fifth order. Each harmonic could appear with positive or negative interaction signs, and combinations of up to four concurrent terms were systematically generated, resulting in approximately 87,000 unique frequency interaction cases. This approach captures realistic defects and harmonic interactions while maintaining computational feasibility. Higher-order combinations were omitted, as their likelihood and spectral distinctiveness are low and would not significantly influence defect classification outcomes. We simply annotated the dominant and important peaks detected, which may or may not be due to compound interactions.

5.2. *Spectral analysis for the spindle on the test bench*

Analysis is presented at the representative spindle speed of 19800 rpm, i.e. for a spindle rotational frequency of 330 Hz. Since this is a high-speed spindle, analysis at higher speeds is valid. We also limit our analysis only to one representative direction — the Y-direction in this case. Though the RMS levels in both directions were similar, we observed consistent spectral signatures in the Y-direction, and hence only those results are presented herein. The spectrum at cold start is shown in Fig. 7(a). Change of spectrums with time is shown in Fig. 7(b). And a representative change in the peak magnitude of a dominant defect frequency is tracked and shown in Fig. 7(c).

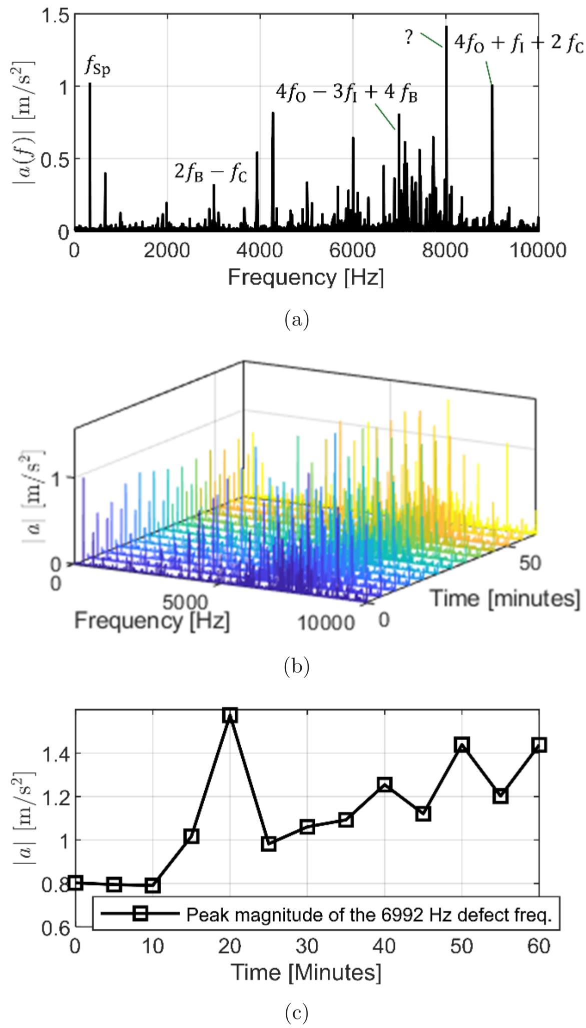

Fig. 7. (a) Spectrum of the motorized spindle mounted on the test bench at cold start, (b) Spectrum changing with measurement time, and (c) Magnitude of one representative peak defect changing with measurement time.

From Fig. 7(a), the spindle fundamental rotational frequency, f_{Sp}, and its harmonics are clearly visible. However, since the harmonics of f_{Sp} have smaller amplitudes than f_{Sp}, no misalignment is detected. Looseness, too, is not detected in this spindle. The frequency spectrum in this case shows multiple peaks corresponding to compound and complex interactions of bearing defects. Combinations of defect frequencies are listed in Fig. 7(a). Though we can classify most of the dominant peaks, we fail to classify the peak at 8012 Hz. This is because spectral methods are not very robust when multiple defects interact with each other, as they do in this case.[17] We also clarify that since our supply frequency is 50 Hz, 8012 Hz is not a harmonic of it. Moreover, the structural resonances of the spindle are usually in the lower frequency range,[20] and hence the peak at 8012 Hz is likely not due to the structure. And, since we sample at 25.6 kHz, the peak is also likely not due to an aliasing effect. Furthermore, the sensor's mounted resonant frequency is >60 kHz, and hence the peak at 8012 Hz is also not due to the sensor's transfer function.

Although defects were detected, no problems were reported with this test bench spindle, i.e. just because we detect defects, it does not mean that the spindle and/or its bearings are damaged. We reiterate that this is a new spindle. And, it is not unusual for new spindles to show defect signatures in their spectra.[7] These signatures are likely due to bearing manufacturing and spindle assembly-related problems.

However, since defects will eventually lead to spindle damage, and since spectral-based diagnosis of damage is based on thresholds of peak magnitudes of defect frequencies, we also track how the vibration spectrum changes with measurement time to distinguish thermal effects from real damage. Figure 7(b) shows the changes in the vibration spectrum with measurement time. And as is evident, there is a change in peak magnitudes of the main defect frequencies at different measurement times. We track one such peak to check how its magnitude changes, and those results are shown in Fig. 7(c). The peak we track corresponds to the compound interaction of the outer race defect with the inner race defect and the ball defect: $-4f_O + 3f_I + 4f_B$. The peak magnitude for this defect increases from 0.8 m/s^2 to around 1.5 m/s^2 at some measurement time. This corresponds to an 87.5% change. This change is more than what was observed in the change in the RMS levels for this spindle at this speed — see Fig. 3(d) for comparisons. The difference can be explained by the energy in the spectrum being divided among all the peaks detected. However, despite the differences between the change in peak magnitudes and the RMS levels, what is obvious from Fig. 7(c), is that the peak magnitudes appear to stabilize between the 2τ and 3τ time-mark, i.e. in between 20 min and 30 min of run time at this speed.

5.3. *Spectral analysis for the spindle on the CNC machine*

Analysis for this spindle type is presented at the representative spindle speed of 15000 rpm, i.e. for a spindle rotational frequency of 250 Hz. Analysis is limited to the X-direction. Figure 8(a) shows the spectrum at the start of the measurement.

The spectrum has a peak corresponding to the spindle rotational frequency, f_{Sp} and peaks corresponding to combinations of defect frequencies. Two such combinations of defect frequencies are listed in Fig. 8(a). One is a compound interaction of the outer race defect interacting with the defects of the inner race, the cage and the ball: $f_O - f_I + 4f_C - f_B$, and another is a combination of the outer race defect interacting with the defects of the inner race and the cage: $-3f_O + 5f_I - 5f_C$. No faults such as misalignment and/or looseness are detected. It should be noted that just because defects are present does not mean that the bearings and/or the spindles

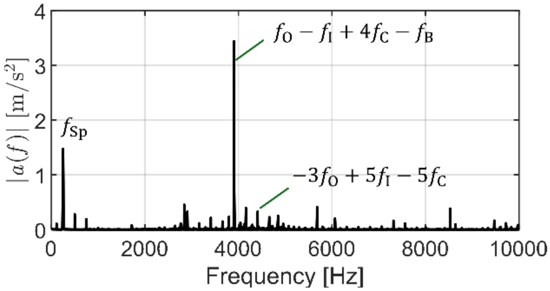

(a)

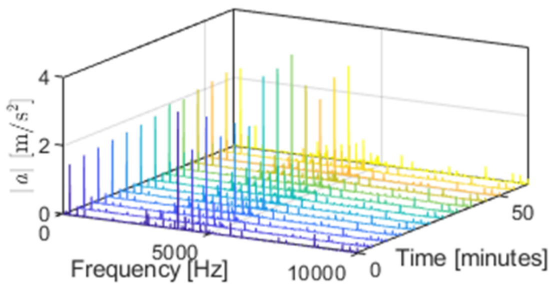

(b)

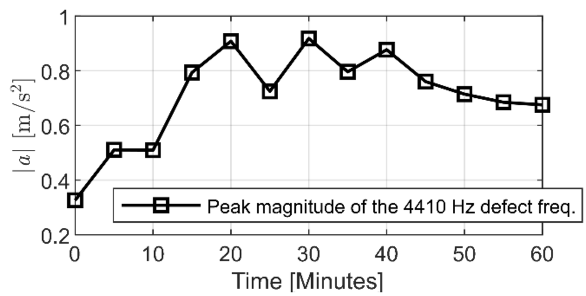

(c)

Fig. 8. (a) Spectrum of the spindle on the milling machine at cold start, (b) Spectrum changing with measurement time, and (c) Magnitude of one representative peak defect changing with measurement time.

are damaged beyond use. Even spindles with new bearings show defects.[7] And, as stated already, this is a sparsely used spindle that was running fine.

Since the spectrum shown in Fig. 8(a) was for the cold-start condition of the spindle, it is important to characterize how/if the spectrum evolves as the spindle thermally stabilizes. That analysis is shown in Fig. 8(b). As is evident, it appears that the peak magnitudes of different defects change with the measurement time. To demonstrate how peak magnitudes change with time, we plot the magnitudes of one representative defect frequency at 4410 Hz ($-3f_O + 5f_I - 5f_C$) changing with time. This is shown in Fig. 8(c). And as is evident, there is a significant change in the peak magnitude of this defect frequency. The peak magnitude changes from 0.3 m/s^2 at cold start and increases to a maximum of 0.9 m/s^2 at several time instances of measurements. Since temperature changes with time, it is evident that the peak magnitude of this defect frequency is also sensitive to a change in temperature. However, as is also evident from Fig. 8(c), the peak magnitude appears to stabilize within an acceptable variation of ±10% starting around 20 min, i.e. around ~2τ for running the spindle at this time.

6. Discussions on Generalizability, Limitations, and Practical Implementation

This section discusses three issues. The first concerns the generalizability of our observations about time, temperature and vibration behavior of spindles. The second issue concerns expected changes in the thermal time constant estimates with changes in the spindle system. The third aspect we discuss pertains to practical guidelines for the implementation of temperature-stabilized vibration measurements.

About observed temperature and vibration behavior: our hypothesis about potential mechanisms responsible for the observed temperature and vibration trends could be better supported by direct measurement of changes in preloads and/or clearances for the spindles we measured. However, since neither the spindle on the test bench and nor the spindle in the CNC machine had preload adjustment mechanisms, and since their preloads were factory-set, relating thermal growth and temperature and vibration stabilization to changing preloads and clearances was not possible. Such exploration would require instrumented spindles, and that analysis could potentially form part of future follow-on research. We also take this opportunity to clarify that it was not possible for us to quantify changes in temperature and vibrations that we observed to changes in preload and/or viscosity of the grease lubricating the bearings. That would require development of analytical models supported by experimentation — something that was beyond the scope of this work, but could be included in the scope of future studies.

Furthermore, since we observe vibration RMS levels and peak magnitudes to change by up to 87%, it might also be worthwhile to explore if the ±10% uncertainty limit as prescribed by the ISO standards is appropriate. Additional experiments may shed more light on this aspect, too.

About the thermal constant estimates: our proposed metric of using the thermal time constant to characterize the temperature-stabilized vibration behavior is anything but universal. Since our estimates suggest that the thermal time constants differ from spindle to spindle, it points to the need for a larger study characterizing the behavior of different spindle types. Such studies could form part of future investigations. Moreover, for the thermal time constant to serve as a practical warm-up metric before diagnostic measurements are undertaken, it might make sense for machine tool manufacturers to evaluate this metric for each of their spindle types

Table 3. Expected changes in thermal time constants with changing spindle parameters.

Parameter	↑ Change	Effect on τ
Spindle mass	↑	τ ↑ (strong)
Bearing heat dissipation	↑	τ ↔ (mostly unchanged)
Ambient convection	↑	τ ↓
Cooling method efficiency	↑ (oil)	τ ↓ (moderate)
Spindle size (diameter)	↑	τ ↑ (very strong)
Speed (air turbulence)	↑	τ ↓ slightly

used on their machines and provide this information to all users for their use in diagnostics and prognostics.

Despite the need for expanded experimental investigations for more robust estimation of the thermal time constants, we still postulate about how the estimate might change with changes in spindle parameters. The spindle's thermal time constant is governed mainly by its thermal mass and cooling effectiveness. Larger rotors and housings possess higher thermal inertia. This will likely result in longer stabilization times. Improved heat rejection — through higher ambient convection, increased internal airflow at higher speeds, or oil-cooled housings, will likely reduce the time constant by raising the effective heat transfer coefficient. We also think that changes in bearing heat generation mainly affect the final temperature, and not the time constant itself. We also think that surface area contributes moderately by enhancing heat dissipation, but this effect is outweighed by the stronger mass dependence. Overall, we postulate that larger spindles will warm up more slowly, while stronger cooling will shorten the thermal response. A summary of these expected changes is tabulated in Table 3 for easy inference. We take this opportunity to clarify that trends in Table 3 are postulations only. These need to be verified and validated, and that can form part of future studies.

About guidelines for practical implementation: To estimate the thermal time constant in factory settings, we recommend placing a temperature sensor near the front bearing or housing and recording 15–20 min of warm-up data. Fitting these data to a first-order exponential will provide a quick in-situ estimate of the thermal time constant, τ, without requiring full stabilization. The fitted τ can then be used to determine when diagnostic vibration measurements should be taken (e.g. after 2τ–3τ). If ambient conditions, spindle speed, or cooling settings change, the short warm-up and curve-fit procedure can be repeated to update τ. This offers a simple and practical way to ensure temperature-stabilized monitoring in everyday machine operation.

7. Conclusions and Outlook

This study establishes that temperature is a dominant contributor to variability in spindle vibration measurements and must be explicitly accounted for in condition monitoring. Experiments on two different spindle architectures showed that vibration RMS levels can vary by up to 40% and defect-peak magnitudes by as much as 87% during warm-up. Such variations exceed typical ISO-permitted uncertainties and can lead to false indications of damage if measurements are taken before thermal stabilization.

To address this, we propose the thermal time constant, τ, obtained by fitting an exponential first-order model to temperature measurements near the spindle bearings. Across all experiments, τ consistently decreased with increasing speed and differed substantially between the compact test-bench spindle and the larger oil-cooled spindle. These differences reflect underlying changes in thermal resistance, thermal capacitance, and cooling effectiveness. Because both RMS levels and defect-peak magnitudes stabilize only after approximately 2τ–3τ, τ provides a reliable and spindle-specific warm-up metric that users can estimate in situ from 15 min to 20 min of early run-up data.

While the present study focuses on two spindles, the methodology is broadly applicable. The thermal time constant is not universal; rather, it should be evaluated for each spindle type — and potentially provided by machine-tool manufacturers as part of diagnostic guidance. Future work should include multi-spindle datasets, instrumented studies linking preload and lubrication changes to observed trends, and a deeper investigation into how temperature-induced spectral variations differ from defect-driven changes. Incorporating τ-based stabilization into diagnostic and prognostic pipelines will significantly improve the reliability of vibration-based spindle health assessment.

Data Availability Statement

The experimental datasets generated and analyzed during this study, including the measured temperature time series and derived thermal time constants for both spindles, are available from the corresponding author upon reasonable request. Processed data used to produce the figures and tables in this paper, as well as the analysis scripts, are archived in the project repository and can also be provided by the authors on request. No proprietary or confidential information is included in the shared data.

ORCID

Mohit Law https://orcid.org/0000-0003-2659-4188

References

1. E. Abele, Y. Altintas and C. Brecher, Machine tool spindle units, *CIRP Ann. Manuf. Technol.* **59** (2010) 781–802, doi:10.1016/j.cirp.2010.05.002.
2. H.-C. Möhring, P. Wiederkehr, K. Erkorkmaz and Y. Kakinuma, Self-optimizing machining systems, *CIRP Ann.* **69** (2020) 740–763, doi:10.1016/j.cirp.2020.05.007.
3. ISO Standard No. ISO/DTR 17243-2, Machine tool spindles — Evaluation of machine tool spindle vibrations by measurements on spindle housing — Part 2: Direct driven spindles and belt driven spindles with rolling element bearings operating at speeds between 600 min^{-1} and 30 000 min^{-1} (2016).
4. ISO Standard No. ISO/TR 17243-1, Machine tool spindles — Evaluation of machine tool spindle vibrations by measurements on spindle housing — Part 1: Spindles with rolling element bearings and integral drives operating at speeds between 600 min^{-1} and 30 000 min^{-1} (2014).
5. A. Rastegari, A. Archenti and M. Mobin, Condition based maintenance of machine tools: Vibration monitoring of spindle units, in *Proc. Annual Reliability and Maintainability Symp.* (*IEEE*, 2017), pp. 1–6, doi:10.1109/RAM.2017.7889683.
6. S. Vafaei, H. Rahnejat and R. Aini, Vibration monitoring of high speed spindles using spectral analysis techniques, *Int. J. Mach. Tools Manuf.* **42** (2002) 1223–1234, doi:10.1016/S0890-6955(02)00049-4.
7. C. De Castelbajac, M. Ritou, S. Laporte and B. Furet, Monitoring of distributed defects on HSM spindle bearings, *Appl. Acoust.* **77** (2014) 159–168, doi:10.1016/j.apacoust.2013.07.008.
8. R. Jamuna, U. Natarajan, A. Elango, S. Jayavel, P. Gokulkumar and V. Shakil, Investigation of spindle thermal expansion in CNC machine, *J. Adv. Manuf. Syst.* **15**(1) (2016) 27–34, doi:10.1142/S0219686716500037.
9. J. Mayr, J. Jedrzejewski, E. Uhlmann, M. Alkan Donmez, W. Knapp, F. Härtig, K. Wendt, T. Moriwaki, P. Shore, R. Schmitt, C. Brecher, T. Würz and K. Wegener, Thermal issues in machine tools, *CIRP Ann.* **61**(2) (2012) 771–791, doi:10.1016/j.cirp.2012.05.008.
10. Y. Li, W. Zhao, S. Lan, J. Ni, W. Wu and B. Lu, A review on spindle thermal error compensation in machine tools, *Int. J. Mach. Tools Manuf.* **95** (2015) 20–38, doi:10.1016/j.ijmachtools.2015.04.008.
11. B. K. Doğan and T. Karaçay, Temperature and vibration condition monitoring of a polymer hybrid ball bearing, *J. Vib. Eng. Technol.* **10** (2022) 2385–2390, doi:10.1007/s42417-022-00601-0.
12. D. S. Truong, B.-S. Kim and S.-K. Ro, An analysis of a thermally affected high-speed spindle with angular contact ball bearings, *Tribol. Int.* **157** (2021) 106881, doi:10.1016/j.triboint.2021.106881.
13. S. Yagyu, S. Shimizu and N. Imai, Mechanism of thermal deviation characteristic in spindle system of machine tools, *Int. J. Automation Technol.* **2**(3) (2008) 191–197, doi:10.20965/ijat.2008.p0191.
14. K. Ogata, *Modern Control Engineering* (Prentice Hall, New Jersey, 1997).
15. M. Mudhasir and M. Law, Perils of vibration RMS-based spindle health monitoring, in *Proc. COPEN13* (2026) (to appear).
16. R. B. Randall, *Vibration Based Condition Monitoring — Industrial, Automotive and Aerospace Applications* (John Wiley and Sons, Hoboken, 2021).

17. M. Law, Finding hidden spindle bearing defect periods using Ramanujan filter banks, *CIRP Ann. Manuf. Technol.* **74**(1) (2025) 477–481, doi:10.1016/j.cirp.2025.04.072.
18. C. Ma, X. Mei, J. Yang, L. Zhao and H. Shi, Thermal characteristics analysis and experimental study on the high-speed spindle system, *Int. J. Adv. Manuf. Technol.* **79** (2015) 469–489, doi:10.1007/s00170-015-6821-z.
19. R. Serrato, M. M. Maru and L. R. Padovese, Effect of lubricant viscosity grade on mechanical vibration of roller bearings, *Tribol. Int.* **40** (2007) 1270–1275, doi:10.1016/j.triboint.2007.01.025.
20. J. J. Zulaika, F. J. Campa and L. N. Lopez de Lacalle, An integrated process-machine approach for designing productive and lightweight milling machines, *Int. J. Mach. Tools Manuf.* **51** (2011) 591–604, doi:10.1016/j.ijmachtools.2011.04.003.